ChemComm

COMMUNICATION

Check for updates

Development of electronically tuneable N-heterocyclic borates†

I. J. Huerfano, [iD] ‡ Evgueni Gorobets, [iD] ‡ Wen Zhou, [iD] Warren E. Piers, [iD] Jeffrey F. Van Humbeck [iD] * and Darren J. Derksen [iD] *

In this contribution, we describe the synthesis and characterization of novel borates constructed with N-heterocyclic arene substituents. Beyond providing comparable electronic and redox properties to their fluoroarene analogues, the use of N-heterocycles allows for facile protonation of aromatic nitrogen atoms, thus providing a framework for tuneable reagents with varying Lewis basicity. The synthesized protonated borates were further examined as Brønstead−Lowry acids through pK_a bracketing and evaluation of the kinetic accessibility of their protons by variable temperature NMR. Finally, we report the synthesis of onium and alkali metal salts of these borates through deprotonation by a variety of bases providing useful starting points for future applications.
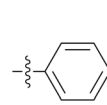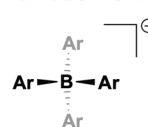
Given the utility of electron poor borates as weakly coordinating anions,[1–3] as activators in polymer catalysis,[4,5] and as electrolytes in energy-related applications,[6] we recognized that novel borates retaining the properties of polyfluorinated borates would be valuable to the chemical community. Combined with the desire to reduce the use of organofluorine compounds,[7–9] we explored the synthesis and properties of tunable N-heterocyclic borates. Based on available Hammett parameters,[10] 4-pyridyl and 5-pyrimidyl have similarities to well-studied pentafluorophenyl substituents but have available sites for further functionalization (Fig. 1).

To sterically shield the Lewis basic sites of the N-heterocycles, we selected *tert*-butyl substituents to flank the nitrogen atoms. 2,6-Di-*tert*-butylpyridine was functionalized with a boronic pinacol ester using Ir catalysis in the presence of 4,4′-di-*tert*-butyl-2,2′-dipyridyl (BBBPY, Scheme 1).[11] Conversion to the corresponding 4-bromopyridine derivative proceeds in 93% yield over 2 steps, which is then lithiated and reacted with boron trifluoride diethyl etherate to produce HB(Py)$_4$ (**1**) upon aqueous workup. ^{1}H- and ^{13}C-NMR spectra of **1** display two sets

Department of Chemistry, University of Calgary, Calgary, AB T2N 1N4, Canada.
E-mail: jeffrey.vanhumbec1@ucalgary.ca, dderksen@ucalgary.ca
† Electronic supplementary information (ESI) available. CCDC 2431948–2431951. For ESI and crystallographic data in CIF or other electronic format see DOI: **https://doi.org/10.1039/d5cc01578b**
‡ These authors contributed equally.

of *tert*-butyl and pyridyl signals in a 3 : 1 ratio as well as a broad signal integrating to a single proton at >9 ppm in the ^{1}H-NMR spectrum, consistent with a three-fold symmetric borate with one of the four pyridyl groups protonated. This assignment is confirmed by structural characterization using single-crystal X-ray diffraction where no cation is observed and the pyridinium proton is seen substitutionally disordered on the four pyridyl arms. Bond lengths and angles are typical of a tetrahedral aryl borate with a τ_4 value[12] of 0.937 confirming the successful synthesis of **1**. Compound **1** exhibits good solubility in both arene and halogenated solvents as well as polar organic solvents such as tetrahydrofuran (THF).
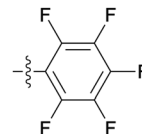
4,6-Dichloropyrimidine was combined with *tert*-butyl lithium, followed by aqueous workup and oxidation with DDQ. Hydrogenation of the resulting 2-*tert*-butyl pyrimidine, followed by bromination, yielded the 5-bromo pyrimidine amenable to formation of a Grignard reagent that reacted efficiently with boron trifluoride diethyl etherate to produce Mg[B(Pm)$_4$]$_2$ (**2**). While **2** can be isolated as the magnesium borate salt, demonstrating remarkable stability in air and water, the pyridyl borate, **1**, is isolated in its protonated form, rather than the lithium salt after aqueous workup.

Previous work

$\sigma_{meta} = 0.06$
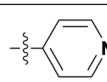$\sigma_{para} = -0.01$

$\sigma_{meta} = 0.26$
$\sigma_{para} = 0.27$
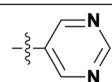
This work

$\sigma_{meta} = 0.27$
$\sigma_{para} = 0.44$

$\sigma_{meta} = 0.28$
$\sigma_{para} = 0.39$

Fig. 1 Comparison of Hammett parameters of aryl and heteroaryl substituents.[10]

Scheme 1 Top: Synthesis of 2,6-di-*tert*-butyl pyridine-derived borate **1** (HB(Py)$_4$). Bottom: 2-*tert*-Butyl pyrimidine-derivate borate **2** (Mg[B(Pm)$_4$]$_2$). Right: ORTEP representations of the molecular structures for **1** and **2**. Thermal ellipsoids are shown at 30% probability. Hydrogen atoms and co-crystallized solvent molecules are omitted for clarity.

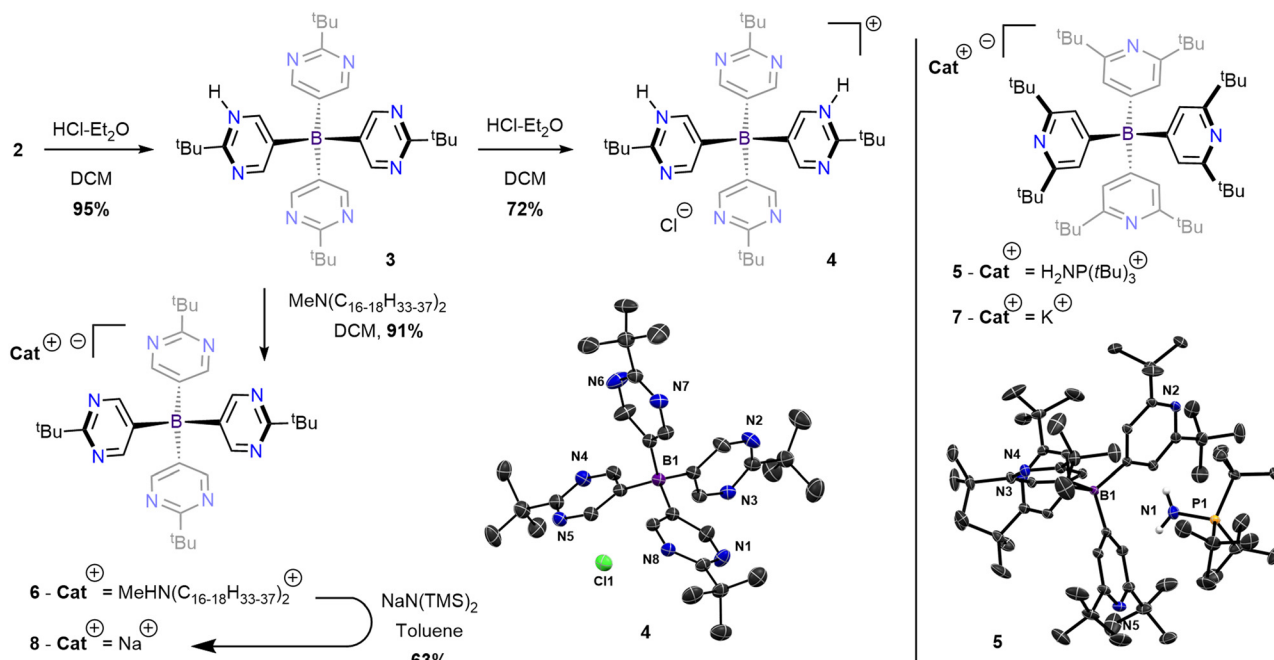^{1}H- and ^{13}C-NMR spectra of the magnesium pyrimidyl borate, **2**, display only a single set of signals, initially suggesting a symmetric borate in solution. Single crystals suitable for X-ray diffraction were grown from a concentrated THF solution layered with pentane and cooled to 5 °C, revealing a solid-state structure containing a magnesium counterion interacting with two pyrimidyl borates through adjacent nitrogen and carbon atoms of one of the pyrimidyl substituents as well as a single THF molecule (Scheme 1, bottom right). The Mg–N distances (2.689 and 2.847 Å) are significantly longer than typical magnesium–nitrogen bonds, falling outside of the sum of the covalent radii,[13] suggesting strong interactions rather than formal bonds. The Mg–O distance of the interacting THF molecule is similarly long (2.773 Å). Long atomic distances may be indicative of lability in the magnesium-borate interactions allowing for dynamic behavior in solution that accounts for the observed symmetric NMR spectra. Similar to **1**, the borate anion of **2** contains bond lengths and angles typical of tetrahedral aryl borates with a τ_4 value of 0.976. For direct comparison to **1**, compound **2** was reacted with 1 equivalent of 1 M HCl/Et$_2$O targeting the analogous protonated pyrimidyl borate, HB(Pm)$_4$ (**3**; Scheme 2). The ^{1}H-NMR spectrum of **3** exhibits a single set of *tert*-butyl and pyrimidyl peaks slightly shifted from the starting material, suggesting successful protonation of the borate. The observed 4-fold symmetry and absence of an observable pyrimidinium proton indicates that this acidic proton is highly fluxional at room temperature

(*vide infra*). In contrast to **1**, compound **3** shows sparing solubility in arene solvents, but is highly soluble in halogenated solvents and moderately soluble in THF.

Compound **3** can be further reacted with an additional equivalent of HCl/Et$_2$O (Scheme 2) to form the doubly protonated chloride salt, [H$_2$B(Pm)$_4$]Cl (**4**). Single crystals of **4** suitable for X-ray diffraction were grown from a concentrated methylene chloride solution layered with pentane and cooled to 5 °C. The solid-state structure shows a borate with protonated pyrimidyl substituents where the two protons are substitutionally disordered across all four arms, analogous to **1** (Scheme 2). Further, the structure contains a chloride anion with a close contact of 2.961(3) Å with one of the protonated nitrogen atoms indicating a hydrogen bonding interaction[14] and confirming the cationic character of the doubly protonated borate. Bond lengths and angles are typical of a tetrahedral aryl borate with a τ_4 value of 0.955. As expected for chloride salts, **4** shows drastically decreased solubility in organic solvents with only modest solubility in methylene chloride (DCM) but can be dissolved in highly polar solvents including dimethyl sulfoxide (DMSO). Like **3**, the ^{1}H- and ^{13}C-NMR spectra show only a single set of peaks indicating fluxional acidic protons. Due to the unique ability of the synthesized pyridyl and pyrimidyl borates to be protonated at their ring nitrogens, we sought to probe their Brønstead–Lowry acid character. Many borate-based acids, most notably Brookhart's Acid, have seen applications in synthesis for the delivery of a proton and weakly-coordinating

Scheme 2 Synthesis of onium borate salts **5** and **6**. Synthesis of alkali metal borate salts **7** and **8**. ORTEP representation of the molecular structure for **4** and **5** thermal ellipsoids are shown at 30% probability. Hydrogen atoms substituents are omitted for clarity.

anion,[15] but most often in their aqueous (hydronium cation) or ethereal (secondary oxonium) forms.

As the formation of water or ethers can be counterproductive to stable cation formation upon proton transfer, a directly protonated borate-acid may serve as a better alternative for some applications. Further, the lack of separate acidic cations can provide a more atom economic reaction overall. The Brønstead–Lowry acidic character of **1** and **3** were evaluated through pK_a bracketing experiments with a variety of neutral organic bases. Through these experiments it was determined that the deprotonated pyridyl borate is moderately basic as **1** shows no reactivity with tertiary amines, but can be deprotonated by stronger organic bases with a pK_a (MeCN scale) between 18.8 (*N*,*N*-diisopropylethylamine) and 21.7 ([−]-spartein).[16] For comparison, **1** is less acidic than lutidinium (a common proton source in catalysis; pK_a = 14.2 MeCN scale) suggesting a possible coulombic component in addition to the effect of an electron donating borate substituent in the *para*-position.[17] As expected, the pyrimidyl borate, **3**, shows greater acidity relative to its pyridyl congener with a pK_a bracketed between 15.07 (imidazole) and 18.8 (triethyl amine). The increased acidity results from the greater nitrogen content of the aromatic ring as well *meta*-positioning of the nitrogen atom relative to the carbon-boron bond.[18] As pK_a is a thermodynamic property, we also sought to evaluate the kinetic accessibility of the proton on the pyridyl and pyrimidyl borates through variable-temperature ^{1}H-NMR experiments using dynamic self-exchange processes as an evaluator of proton mobility (see Fig. S33 and S34, ESI†). The pyridyl borate, **1**, shows no coalescence up to 100 °C in toluene maintaining its two sets of peaks in a 3 : 1 ratio, indicating there is a high barrier to proton

transfer between two separate borates. This observation likely results from the two large *ortho tert*-butyl groups. In contrast, **3** exhibits fast exchange at room temperature (*vide supra*) which can be de-coalesced at low temperature to give two sets of peaks analogous to **1**. The coalescence point for **3** was determined to be at −57 °C in DCM indicating a low barrier for proton transfer. Having evaluated the Brønstead–Lowry acidic character of **1** and **3**, we next synthesized onium and alkali metal salts of the pyridyl and pyrimidyl borates. Based on the bracketed pK_a values and steric protection around the pyridinium proton, **1**, was reacted with equimolar tris(*tert*-butyl)phosphinimine (HNP^{t}Bu$_3$) and allowed to stir at room temperature in toluene for 18 hours (Scheme 2, right). In this time, precipitation of colorless crystals is observed. Upon removal of solvent *in vacuo*, [H$_2$NP(^{t}Bu)$_3$][BPy$_4$] (**5**) is isolated as a white microcrystalline powder in quantitative yield. ^{1}H- and ^{13}C-NMR spectra of the isolated solid show that the product contains a completely symmetric pyridyl borate in solution with only one set of signals. Further, ^{1}H- and ^{31}P-NMR confirm the presence of the phosphiniminium counter cation. Single crystals of **5** suitable for X-ray diffraction were grown from a concentrated toluene solution layered with pentane and confirms the successful synthesis of the targeted phosphiniminium borate (Scheme 2). The bond lengths and angles of **5** are all consistent with a tetrahedral borate anion with a τ_4 value of 0.946. Notably, the acidic protons of the phosphiniminium cation do not hydrogen bond with the pyridyl nitrogen atoms of the borate but instead are directed towards the borate center itself. As **3** can be deprotonated by tertiary amines, it was instead reacted with one equivalent of a hydrophobic amine, containing two long aliphatic (C$_{16}$–C$_{18}$) chains, in benzene at room

temperature for 6 hours (Scheme 2, left). Over the course of the reaction, the mixture changed from a light orange suspension, due to the low solubility of **3** in aromatic solvents, to a homogeneous off-white solution. The final ammonium borate product, **6**, was isolated as a tacky off-white solid after removing the solvent by lyophilization.

The ^{1}H-NMR spectrum of **6** is consistent with a completely symmetric borate containing a tertiary ammonium cation. Compared to the starting amine, the α-methyl/methylene protons are now further split into doublets due to coupling with the acidic proton bound to the nitrogen center and supporting the assigned structure (see Fig. S22, ESI†). Similar to the discussed onium salts, alkali metal salts of the pyridyl and pyrimidyl borates are also accessible through use of an appropriate strong base. Compound **1** was deprotonated using benzyl potassium (KBn) in THF or dimethoxyethane (DME) to give KBPy$_4$, **7**, as white powder after removal of solvents *in vacuo* (Scheme 2, right). Compound **7** is only soluble in ethereal solvents (diethyl ether, THF, and DME) but dissolves in arene or halogenated solvents with addition of a small amount of ethereal solvent additive. Additionally, **7** can be recrystallized from DME to give the highly soluble K(DME)$_n$BPy$_4$ (**7·DME$_n$**) where n = 1–4 and must be quantified by ^{1}H-NMR. The ^{1}H- and ^{13}C-NMR spectra of **7·DME$_n$** confirm their identity as separated ion pairs showing only one set of borate signals, regardless of the number of DME ligands. Due to the poor solubility of **3** in non-halogenated solvents, its deprotonation by strong alkali metal bases leads to inconsistent results. As these bases are incompatible with DCM or chloroform, **3** was first converted to **6** *in situ* then reacted with sodium hexamethylsilazide (NaHMDS) in toluene to give the corresponding sodium salt, **8** (Scheme 2, left). The ^{1}H- and ^{13}C-NMR spectra of **8** are very similar to that of **2** showing only a single set of borate peaks suggesting weak sodium association to the borate and fluxional behavior in solution. The redox properties of these anions were evaluated through cyclic voltammetry (CV) to determine their resistance to oxidation by possible redox-active cations. CV of **7** in THF shows a single irreversible oxidation process with a peak potential approaching the solvent window of THF around 1.8 V *vs.* Fc/Fc$^+$. This oxidation potential is comparable to the redox potential of B(C$_6$F$_5$)$_4$$^-$ and B[C$_6$H$_3$(CF$_3$)$_2$]$_4$$^-$ suggesting the pyridyl borate may be useful as a counteranion from a redox perspective.[19–21] Similarly, the CV of **2** in DCM shows a quasi-reversible oxidation occurring at 1.7 V *vs.* Fc/Fc$^+$ also demonstrating the pyrimidyl borates possible utility as a redox-resistant counteranion.

We have demonstrated that borates with heterocyclic substituents are synthetically accessible on gram scale. These compounds have tuneable properties compared to pentafluorophenyl substituents with respect to basicity and electrochemistry. Given

the broad applications of borates, we anticipate that this novel family of compounds will be useful to the chemical community.

This work was conceptualized by DJD, JFVH and WEP. Synthesis and characterization were completed by IJH and EG. Crystallography was completed by WZ. Writing of original draft was completed by DJD and IJH with reviewing and editing by all authors.

Conflicts of interest

There are no conflicts to declare.

Data availability

The data supporting this article have been included as part of the ESI.† Crystallographic data for **1**, **2**, **4**, and **5** has been deposited at the CCDC under 2431948–2431951.

Notes and references

1 S. D. Ittel, L. K. Johnson and M. Brookhart, *Chem. Rev.*, 2000, **100**, 1169.
2 I. M. Riddlestone, A. Kraft, J. Schaefer and I. Krossing, *Angew. Chem., Int. Ed.*, 2018, **57**, 13982.
3 S. H. Strauss, *Chem. Rev.*, 1993, **93**, 927.
4 J. F. Van Humbeck, M. L. Aubrey, A. Alsbaiee, R. Ameloot, G. W. Coates, W. R. Dichtel and J. R. Long, *Chem. Sci.*, 2015, **6**, 5499.
5 S. Fischer, J. Schmidt, P. Strauch and A. Thomas, *Angew. Chem., Int. Ed.*, 2013, **52**, 12174.
6 Z. G. Huang, S. N. Wang, R. D. Dewhurst, N. V. Ignat'ev, M. Finze and H. Braunschweig, *Angew. Chem., Int. Ed.*, 2020, **59**, 8800.
7 M. G. Evich, M. J. B. Davis, J. P. McCord, B. Acrey, J. A. Awkerman, D. R. U. Knappe, A. B. Lindstrom, T. F. Speth, C. Tebes-Stevens, M. J. Strynar, Z. Wang, E. J. Weber, W. M. Henderson and J. W. Washington, *Science*, 2022, **375**, eabg9065.
8 I. T. Cousins, J. C. Dewitt, J. Glüge, G. Goldenman, D. Herzke, R. Lohmann, M. Miller, C. A. Ng, M. Scheringer, L. Vierke and Z. Wang, *Environ. Sci.: Processes Impacts*, 2020, **22**, 1444.
9 J. Scholl, J. Lisec, H. Haase and M. Koch, *Anal. Bioanal. Chem.*, 2024, **416**, 6405.
10 C. Hansch, A. Leo and R. W. Taft, *Chem. Rev.*, 1991, **91**, 165.
11 L. Zeqing, L. Zhibin, W. Yuqiang and Y. Pei, *Res. Chem. Intermed.*, 2013, **39**, 1917.
12 L. Yang, D. R. Powell and R. P. Houser, *Dalton Trans.*, 2007, 955.
13 B. Cordero, V. Gómez, A. E. Platero-Prats, M. Revés, J. Echeverría, E. Cremades, F. Barragán and S. Alvarez, *Dalton Trans.*, 2008, 2832.
14 T. Steiner, *Acta Crystallogr., Sect. B*, 1998, **54**, 456.
15 M. Brookhart, B. Grant and A. F. Volpe Jr, *Organometallics*, 1992, **11**, 3920.
16 S. Tshepelevitsh, A. Kütt, M. Lõkov, I. Kaljurand, J. Saame, A. Heering, P. G. Plieger, R. Vianello and I. Leito, *Eur. J. Org. Chem.*, 2019, 6735.
17 T. Taniguchi, *Chem. – Eur. J.*, 2022, **28**, e202104333.
18 J. Spanget-Larsen, *J. Chem. Soc., Perkin Trans. 2*, 1985, 417.
19 S. B. Beil, S. Möhle, P. Enders and S. R. Waldvogel, *Chem. Commun.*, 2018, **54**, 6128.
20 W. E. Geiger and F. Barrière, *Acc. Chem. Res.*, 2010, **43**, 1030.
21 S. H. Dempsey, A. Lovstedt and S. R. Kass, *J. Org. Chem.*, 2023, **88**, 10525.